Polymer-Leather Composites. I. Process and Location Study for the Deposition of Selected Acrylate Monomers by Polymerization into Chrome-Tanned Cattlehide

EDMUND F. JORDAN, JR., BOHDAN ARTYMYSHYN, ALFRED L. EVERETT, MARY V. HANNIGAN, and STEPHEN H. FEAIRHELLER,
Eastern Regional Research Center, Philadelphia, Pennsylvania 19118*

Synopsis

Three acrylate monomer systems were deposited by redox emulsion polymerization at room temperature into the fibrous matrix of 2-mm-thick chrome-tanned cattlehide over a wide range of composition. Polymer not bound to the matrix was separated by hot benzene extractions. Monomers used were methyl methacrylate, a mixture of *n*-butyl acrylate and methyl methacrylate and *n*-butyl acrylate, each selected to produce composites having wide variation in glass-transition temperature. The same three systems were introduced into the free space of leather by bulk and solution polymerization. All conversions were close to 100%. When the emulsion technique was used, with feed composition variable, overall deposition efficiency depended on the characteristic rate of deposition for the individual acrylate monomers. Observed orders in deposition rate and overall efficiency were: methyl methacrylate > comonomer > *n*-butyl acrylate. However, specific deposition efficiencies declined roughly monotonically with feed or time increase, but maintained the same order. Microscopic examination of thin sections revealed polymer only in the outer region of the leather cross section. Information on polymer location and its influence on specimen thickness for composites prepared by both emulsion and solution methods of deposition were obtained by correlating experimental densities with theoretical density–composition curves for various assumed models. The foregoing, together with observations of greatly reduced grafting frequency, in view of the maximum theoretically attainable, made a dominant grafting mechanism unattractive. A mechanism involving diffusion controlled monomer transport to occluded radicals in localized polymer deposits was suggested as an alternative.

INTRODUCTION

This article and several that follow[1a,1b] provide a systematic study of the process by which selected acrylate polymers are deposited in leather. The mechanical properties of the composites investigated will be presented in a later article.[1c] The polymerization of monomers in collagen and leather has received scant attention in reviews[2–4] compared to that in cotton,[5–8] wool,[9–11] and natural fibers in general,[12] reflecting reduced activity in this field. In contrast, the physics and chemistry of collagen and leather have been extensively treated, with reviews available on classical protein chemistry,[13a] practical leather manufacture,[14] materials science,[15] and solid-state physics.[16] Although the bulk of the literature on the treatment of wool and cotton by polymerization of monomers within their fibers implies that most of the bound polymer is truly grafted,[5–11]

* Agricultural Research, Science and Education Administration, U. S. Department of Agriculture.

Journal of Applied Polymer Science, Vol. 25, 2621–2647 (1980).
© 1980 John Wiley & Sons, Inc.
0021-8995/80/0025-2621$02.70

some doubt remains as to whether the unextractable polymer is covalently bonded or merely entrapped.[9,12] Most of the work involving similar treatment of leather by polymerizing monomers has been interpreted to require a controlling grafting mechanism to account for the considerable amount of bound polymer formed. This was true whether water soluble or insoluble monomers were polymerized in soluble or insoluble powdered collagen,[17–20] in intact pickled goat skins,[21,22] or chrome-tanned Nigerian sheepskins[23–26] using ceric ion,[17–23] potassium persulfate–sodium bisulfite redox initiator[23–26] or other[27] techniques. Sheepskin composites were characterized by end group analysis,[28] unextractable networks were prepared,[29] and graft molecular weights were controlled by chain transfer.[30] Kudoba has employed nonradical means as well as radical formation through photoinitiation to prepare an extensive list of collagen polymer composites (see ref. 4). Finally, ratskins and bone have been modified by use of an exceptionally large number of acrylate and other types of monomers and polymers.[4,31]

A major aim of this work and that which follows[1a,1b] is concerned with determining whether a dominant grafting mechanism is responsible for most of the bound polymer produced in leather composites or whether the unextractable polymer is crosslinked or physically entrapped in confined regions.[9,12] Consequently aspects of deposition yield, efficiency and bound polymer frequency as functions of polymer composition are emphasized. Bound polymer efficiency must remain large, even as feed composition approaches unity, to maintain the high graft frequency that must characterize a controlling grafting mechanism. Toward these aims new information is presented on the process by which three selected acrylate monomer systems are incrementally deposited and bound to 2-mm-thick panels of chrome-tanned cattlehide as functions of monomer concentration and time. A standard persulfate-bisulfite procedure, developed at this laboratory[23–26] as a practical process for modifying leather properties, is used here with only minor modification. A new process, in which polymer is deposited, unbonded, into the pore structure of leather is described. Finally, the role of composite density in characterizing matrix polymer deposition is treated in considerable detail.

EXPERIMENTAL

Starting Materials

The leathers used were commercial grain split 5-oz. (0.23-cm-thick) chrome-tanned blue stock (water wet) cattlehide used in shoe uppers. These were cut in panels (8.9 × 15.2 × 0.235 cm) from the full hide (short dimension parallel to the backbone with 10-cm borders) starting in the butt and progressing to the shoulders crisscross to the belly region. To minimize the effect of location on properties[32a] adjacent panels were paired as controls with all treated samples. The panels were extracted four times for 45 min each with acetone (5 cm^3/g wet) dried and analytically weighed after equilibrium over calcium sulfate and their density determined. Commercial monomers, methyl methacrylate (MMA), *n*-butyl acrylate (BA), and a fixed composition *n*-butyl acrylate (0.591 weight fraction), methyl methacrylate (0.409 weight fraction), monomer mixture (BA + MMA) from commercial sources, were freed of inhibitor by alkali extraction.

The glass transition temperatures T_g for the respective polymers were MMA, 105°C (ref. 33); BA + MMA, 10.5°C (ref. 34); and BA, −55°C.[33]

Composite Preparation Procedures

In the emulsion procedure, each panel (~16 g) after overnight equilibration under nitrogen in water (16 cm^3/g dry) was padded dry, corrected for salt loss in the soak, and tumbled in sealed jars for 30 min with the redox initiator dissolved in the aqueous phase. The monomer was then introduced under nitrogen and the mixture tumbled for another 24 hr at room temperature. Polymerization conversions were usually 100%. The treated panels were water washed and extracted four times with hot methanol (16 cm^3/g initial dry weight) and, after drying at ambient and over calcium sulfate, the deposited polymer was determined gravimetrically; some compositions were checked using Kjeldahl nitrogen analysis. The aqueous emulsion (float) was coagulated in sodium chloride and methanol and extracted with hot methanol. Homopolymer was removed from selected panels by use of three hot benzene extractions (50 cm^3/g) for 24 hr, except that the first extraction was for three days. For multibatch deposition (text) this polymerization procedure was repeated several times. A complete material balance was maintained throughout the work.

Quantities used were water, 5/1 based on dry leather; monomer, variable; potassium persulfate, generally 4 mole % based on monomer; $NaHSO_3/K_2S_2O_8$, 0.5 except MMA, 0.2; Triton X100, 1.03%, 2 cm^3/g based on wet leather. For rate determination strips 2.6 × 7.3 × 0.235 cm were used and the initiator pretreatment was eliminated.

In the solution polymerization procedure leather panels saturated with monomer or incrementally varied benzene–monomer mixtures, adjusted to regulate the feed composition, and containing 3 mole % azo-bis-isobutyronitrile (AIBN) 2 mole %, MMA) were polymerized in sealed systems in nitrogen at 60°C for 24 hr to 100% conversion. The excess monomer was separately polymerized. Panels and polymer were extracted in methanol at room temperature and dried.

Physical Properties and Staining Procedures

Apparent densities of composites and untreated controls were calculated by measurement of their volumes; machine cut specimens gave similar densities. Real densities were obtained with a model 1302 Micrometric Helium-Air Pycrometer. Density of the neat homopolymers and copolymer were estimated from a group additivity method[35] and some were checked with the helium air pycrometer. Densities, g cm^{-3}, were MMA, 1.146; BA + MMA, 1.103; BA, 1.072. A staining technique employing Oil Red O for 6 hr on thin sections (50 μm) was used to monitor the polymer that deposited in cattlehide, unlike sheepskins,[23–26] in layers exclusively in the grain (top) and split corium portions (bottom) of the cross sections, leaving the center section polymer-free. Bound polymer was isolated from the composites by digesting small panels with excess 6*N* hydrochloric acid at 90°C for 8 and 18 hr at room temperature. Lack of color change on repetition of the process for 1–2 hr was taken to yield complete hydrolysis. Drying followed many water washes; nitrogen values on the isolated polymer were

negligible. The MMA polymer replicas retained their leather appearance.[1b] Molecular weights were obtained at 37°C in toluene using a Mecrolab* membrane osmometer, model 501.

Definitions

In this work mole fraction is designated m, and weight fraction w. Subscripts are 1, leather; 2, polymer; d, deposited polymer; b, bound polymer; c, critical; max, maximum; a, apparent; r, real; p, synthetic polymer (or copolymer); f, float; e, extracted. Quantities W and V represent specimen weight in g and volume in cm^3, respectively. Polymers deposited in the leather are identified by their monomers; MMA, BA + MMA, BA, respectively.

Other definitions used are given below. Deposited and bound polymer fraction as percent[36]

$$\text{percent deposited} = [(W_2 + W_1) - W_1]/W_1 \times 100 = (W_2/W_1) \times 100 \quad (1a)$$

$$\text{percent bound} = (W_2 - W_e)/W_1 \times 100 = W_{2b}/W_1 \times 100 \quad (1b)$$

deposited and bound polymer efficiency fraction[37]

$$\epsilon_d = W_d/W_T \quad (2a)$$

$$\epsilon_b = W_b/W_T \quad (2b)$$

bound polymer frequency fraction[36]

$$F_b = \frac{\overline{M}_{n\text{collagen}}/w_1}{\overline{M}_{n2}/w_b} = \frac{w_b\overline{M}_{n\text{collagen}}}{w_1\overline{M}_{n2}} \quad (3)$$

W_T is the total weight of polymer obtained. The molecular weight ($\overline{M}_n$, $\overline{M}_w$) of collagen was taken as 300,000.[13a,15] Curve fitting was done on an IBM 1130 computer.

RESULTS AND DISCUSSION

General Features

Table I lists selected data on polymer–leather composites prepared by the emulsion polymerization method with each acrylate monomer and mixtures of the two. Feed weight fractions (column 2) and composite compositions (column 3) varied over a wide range (Sections A–C). Differing workup procedures account, in part, for the large number of samples prepared, of which only selections appear in the table. For example, similar composites to those listed here were isolated either by air drying or methanol extracting followed by drying. In addition, composites produced by varying time at a fixed feed composition $w_{2\text{feed}}$, 0.5 were introduced for comparison (Section D).

Results in Table I, in harmony with those of most other investigators,[7,9] generally show steady increases in deposited and bound polymer composition with $w_{2\text{feed}}$. However, conversion weight fractions for polymer formed in the external aqueous layer (float) w_f tended to attain high values compared to that deposited

* Reference to brand or firm name does not constitute endorsement by the U.S. Department of Agriculture over others of a similar nature not mentioned.

beyond a critical $w_{2\text{feed}}$, characteristic of the monomer system, except for MMA. Consequently, deposition and bound efficiencies ϵ_i (columns 8 and 9), decreased, the magnitude of the decrease being dependent on the monomer used. The order in deposition and rate of deposition was MMA > BA + MMA > BA. Bound polymer was usually considerably less than that deposited. Rate data at fixed feed composition (Section D) followed the trends of Sections A–C, as would be expected. All densities appear to be monotonic functions of composition or time.

Data on bulk or solution deposition (Table II) resembled that for deposition from emulsion except that densities were uniformly higher for the same w_2. Molecular weights for the free polymer systems in Table II (column 7) tended to be low, probably reflecting the high initiator (AIBN) concentrations required for high conversions in the composites (~2 to 3 mole %). Molecular weight distribution of all polymers was apparently broad because fractions soluble in methanol were found for BA and BA + MMA composites. Molecular weights for polymer extracted from selected composites with benzene (last column) were higher than those in column 7. This suggests that a Tromsdorff effect was present when bulk polymer was produced in the tight confines of the leather matrix. Reduction in molecular weights with benzene dilution, approaching values in column 7, would be expected in view of literature trends.[30,38] Polymer could not be completely extracted from at least two of these composites (Table II, footnote). AIBN was selected because it is a poor graft initiator.[39] Either entangled polymer was unremovable from the fine structure, or popcorn, or some other type of crosslinked polymer was formed.

A more detailed treatment of some of the emulsion data in Table I is presented in the sections that follow. Further discussion of the bulk or solution composites is reserved for the density section.

Feed and Rate Effects

Figure 1 shows percent deposition and bound polymer curves plotted as a function of the monomer concentration used (based on water) for all three acrylate monomer systems prepared by the emulsion method. Solid points are multibatch deposition points. While the extent of deposition appears to continue indefinitely, dependence on monomer concentration increased rapidly beyond 100% deposition. However, in this work, multibatch deposition was usually the only practical way to obtain exceptionally high yields (Table I). In Figure 2 weight fractions of polymer in the composite w_2 are plotted against the weight fraction of the monomer in the feed $w_{2\text{feed}}$. The slopes provide estimates of overall deposition efficiency, designated D_e, for each monomer system. Thus

$$w_2 = D_e w_{2\text{feed}} \tag{4}$$

The maximum D_e is 1, the dotted line; values of D_e are presented in Table III for the three systems.

In contrast, polymer deposited as a function of time is shown in Figure 3(A), for all three systems. From the slopes the rates, designated R_d, were estimated (Table III). Percent conversion–time curves accounting for all polymers formed in each system, are shown in Figures 3(B)–3(D), and are compared with rates in the absence of leather (dotted lines). The rate of deposition of methyl

TABLE I

Compositions, Matrix Distributions, Deposition Efficiencies, Densities, and Rates for a Selection of the Emulsion Polymerized Leather Composites[a]

Experiment No.	Monomer in feed, w_{2feed}[b]	Composite composition: Polymer deposited w_2[b]	Composite composition: Polymer bound w_2[b]	Leather matrix distribution: Deposited (%)	Leather matrix distribution: Bound (%)	Float conversion fraction, w_f	Deposition efficiency: ϵ_d[c]	Deposition efficiency: ϵ_b[c]	Density,[d] g cm^{-1}: Deposited	Density,[d] g cm^{-1}: Bound	Fraction homopolymer in composite[e] w_h
				(A) Poly(methyl methacrylate)-leather composites, benzene extracted							
1	0.103	0.0777	0.0223	8.50	2.41	0	1.0	0.28	0.549	0.536	0.716
2	0.200	0.180	0.0894	21.9	9.82	0	1.0	0.45	0.660	0.563	0.552
3	0.301	0.249	0.203	33.2	25.5	0	1.0	0.77	0.700	0.599	0.232
4	0.401	0.396	0.335	60.9	50.3	0.092	0.90	0.75	0.743	0.643	0.174
5	0.500	0.443	0.447	79.4	80.7	0.065	0.93	1.0	0.805	0.769	0
6	0.667	0.598	0.160	149.0	19.2	0.013	0.99	0.092	0.598	0.419	0.871
7	0.750	0.748	0.212	296	26.9	0.052	0.95	0.086	0.748	0.397	0.909
				(B) Poly(n-butyl acrylate-co-methyl methacrylate)-leather composites, benzene extracted							
8	0.103	0.0742	0.0338	8.01	3.50	0.229	0.75	0.33	0.622	0.618	0.563
9	0.200	0.1820	0.140	22.2	16.3	0.121	0.88	0.65	0.665	0.609	0.265
10	0.301	0.294	0.260	41.5	34.8	0.042	0.96	0.80	0.601	0.572	0.162
11	0.401	0.327	0.279	48.5	38.6	0.282	0.72	0.57	0.614	0.573	0.205
12	0.500	0.372	0.306	59.1	44.1	0.414	0.59	0.44	0.712	0.616	0.254
13	0.750	0.528	0.353	111.9	54.6	0.596	0.38	0.19	0.812	0.605	0.512
				(C) Poly(n-butyl acrylate)-leather composites, benzene extracted							
14	0.103	0.0416	0.0114	4.34	1.15	0.271	0.39	0.086	0.612	0.605	0.749
15	0.200	0.123	0.0629	14.1	6.71	0.251	0.57	0.26	0.646	0.619	0.546
16	0.300	0.141	0.0853	16.4	9.33	0.442	0.90	0.49	0.597	0.599	0.461
17	0.400	0.223	0.173	28.8	21.0	0.443	0.81	0.57	0.621	0.575	0.308
18	0.500	0.340	0.259	50.5	35.0	0.506	0.49	0.33	0.680	0.587	0.343
19	0.667	0.193	0.0353	23.9	3.66	0.847	0.12	0.018	0.721	0.580	0.731
20	0.750	0.333	0.0616	50.0	6.56	0.838	0.16	0.015	0.703	0.562	0.869

(D) Poly(n-butyl acrylate-co-methyl methacrylate)[f]-leather composites, benzene extracted; rates

	Time, min[g]										
21	30	0.0761	0.0496	8.23	5.22	0	1.0	0.85	0.540	0.559	0.366
22	60	0.123	0.0661	14.0	7.08	0.023	0.98	0.50	0.542	0.567	0.494
23	90	0.208	0.0990	26.3	11.0	0.048	0.85	0.36	0.592	0.544	0.581
24	105	0.251	0.147	33.5	17.3	0.037	0.90	0.47	0.617	0.539	0.483
25	120	0.253	0.125	33.9	14.3	0.035	0.90	0.38	0.593	0.515	0.578
26	150	0.300	0.172	42.8	20.7	0.092	0.82	0.40	0.627	0.503	0.516
27	180	0.371	0.242	59.0	31.9	0.154	0.79	0.43	0.637	0.511	0.460
28	195	0.387	0.259	63.0	35.0	0.178	0.78	0.43	0.657	0.513	0.445
29	210	0.523	0.192	47.6	23.8	0.062	0.88	0.44	0.625	0.514	0.500
30	240	0.412	0.260	70.0	36.3	0.288	0.71	0.37	0.762	0.536	0.482

[a] This is only a partial list and represents typical data obtained on the emulsion polymerized composites studied in this work. Data on the balance (~70 experiments) are included as components in the various graphs and tables below.

[b] w_i is weight fraction. Subcript 2 designates polymer. Monomer bears the additional designation, feed.

[c] In this work, subscript d refers to deposited polymer; subscript b bound polymer.

[d] In some cases two determinations were made and each plotted.

[e] $w_h = 1 - (W_b/W_d)$.

[f] Copolymer composition was n-butyl acrylate, mole fraction 0.530; weight fraction 0.591.

[g] Weight fraction $w_{2\text{feed}}$ was 0.50.

TABLE II
Compositions, Efficiencies, Densities, and Number-Average Molecular Weights of Bulk and Solution Polymerized Leather Composites

Experiment No.[a]	w_{2feed}	Deposited polymer w_2	Deposited polymer %	ϵ_d[b]	Density (g cm^{-3})	$\bar{M}_n$ No leather	$\bar{M}_n$ In leather
			Poly(methyl methacrylate)				
1	0.153	0.0962	10.6	0.63	0.775	19,500	
2	0.205	0.155	18.4	0.76	0.780		
3	0.235	0.189	23.3	0.80	0.793	22,600	
4	0.268	0.234	30.6	0.87	0.874	24,800	
5	0.313	0.292[c]	41.2	0.93	0.948	432,900	
6	0.441	0.397[d]	64.8	0.90	1.036	60,100	241,600
7	0.456	0.423[d]	82.0	0.93	1.081		
8	0.434	0.645[e]	182[e]	—	1.173		
9	0.434	0.701[e]	234[e]	—	1.154		
			Poly(*n*-butyl acrylate-co-methyl methacrylate)				
10	0.172	0.084	9.14	0.49	0.683		
11	0.250	0.195	24.2	0.78	0.807		
12	0.315	0.263	35.7	0.83	0.845		
13	0.306	0.310	44.9	1.0	0.962	88,300[c]	
14	0.455	0.442[e]	79.2	0.97	1.011		190,200
15	0.479	0.467[e]	87.4	0.98	0.975	132,050[c]	
16	0.531	0.543[e]	119[e]	—	1.134		
17	0.521	0.667[e]	201[e]	—	1.107		
			Poly(*n*-butyl acrylate)				
18	0.198	0.143	16.7	0.72	0.747	93,700	
19	0.267	0.223	28.8	0.84	0.877	94,950	
20	0.293	0.250	33.4	0.85	0.904	99,200	
21	0.326	0.281	39.0	0.86	0.936	124,700	
22	0.400	0.346[d]	52.9	0.87	0.951	109,200	210,500

[a] Experiments 6–9, 14–17, and 22 were bulk polymerized; the balance were polymerized in benzene at different concentrations. This table is a partial list of experiments; data for the balance appear in appropriate figures.

[b] Taken here as w_2/w_{2feed}.

[c] Fractions, 0.35 experiment 13 and 0.41, experiment 15, soluble in methanol, had molecular weights of 27,600 and 26,300, respectively.

[d] After benzene extractions for 7 hr at reflux and 24 hr at room temperature the composite compositions were PMMA, w_2 = 0.114, 0.011, and 0.051, respectively; BA + MMA, w_2 = 0.1716; PBA, w_2 = 0.1920.

[e] Prepared by depositing polymer from methyl ethyl ketone solution to bulk polymerized composites and evaporating the solvent.

methacrylate into leather [Fig. 3(B)] was much greater than for neat homopolymerization. The extent of float homopolymerization was minimal over the conversion range. Range of deposition into leather and homopolymerization were essentially the same for BA + MMA [Fig. 3(C)] with float polymer increasing abruptly at around 50% conversion. In contrast, homopolymerization greatly exceeded the rate of deposition for *n*-butyl acrylate [Fig. 3(D)]; float polymers followed the usual Tromsdorff rate effects expected for this type of monomer, but only after a percent conversion of about 30% was reached. The unusual and unexpected behavior for these systems clearly indicates that rates of deposition were dependent either on some specific effective[9] concentration of radicals forming preferentially in the leather matrix that is characteristic of

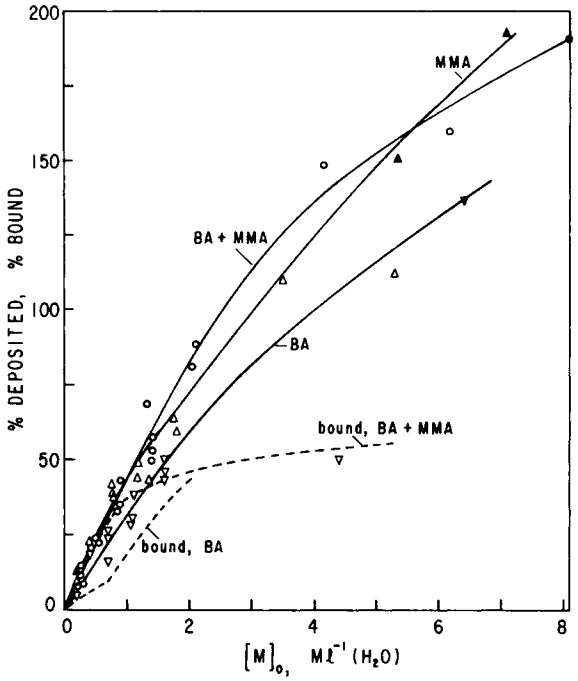

Fig. 1. Effect of initial monomer concentration on deposition and bound polymer yields. Solid points represent multideposition data. Bound MMA curve lies close to the corresponding deposition curve but was omitted for clarity; bound experimental points are omitted.

each system or that polymer latex particles were preferentially removed from the float. Initial concentrations of initiator were similar for all three systems. Rates also appear dependent on the rate of diffusion of monomer through the polymer phase, accounting for the constancy of dW_2/dt for the polymer forming in the leathers. However, the rates of deposition are in reverse order of that expected if the effect of Fickian diffusion on the T_g of the polymer components is considered. Further discussion of these points will be reserved for the next article; it suffices to note here that bound polymer rate of formation was about one-half of that found for the deposited polymer.

The effect on overall rate of polymerization by large increase of polymer in the float, formed at times exceeding 160 min in Figures 3(B)–3(D) is demonstrated in Figure 4(A). These times mark the onset of reduced rates of deposition (dashed lines) for the illustrated dw_2/dt curves, which continue to very long times. Included in the curve fitting are the sums of polymerization times for the multibatch deposition data points (not shown). Clearly for each system there occurs a discontinuous transfer of the main site of polymerization from the fibrous matrix, characterized by the steep curves (solid lines) in the figure, to the float, with only the retention of limited deposition activity (dashed lines). The above observations suggest that the major portion of polymer growth takes place on occluded radicals, where rate is dependent on monomer diffusion up to a saturation level, whereupon the mechanism changes abruptly.

The initial curves (solid lines) in Figure 4(A), for each system follow

$$w_2 = Ft \tag{5}$$

and values of F are given in Table III. The relation between D_e and the rate of

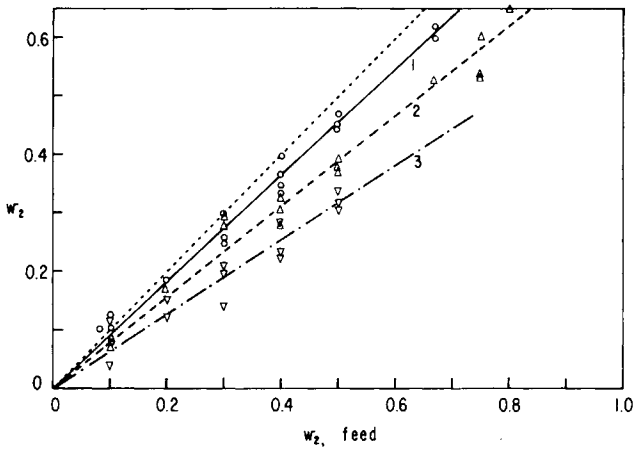

Fig. 2. Weight fraction of polymer deposited w_2 vs. the weight fraction of monomer in the feed $w_{2\text{feed}}$. Curve designations are (1) MMA; (2) BA + MMA; curve (3) BA; dotted line, maximum deposition efficiency, $D_e = 1$.

deposition R_d for the three composite systems [from Fig. 3(A) and Table III] is (Fig. 5)

$$D_e = D_{e0} - C/R_d = w_2/w_{2\text{feed}} \tag{6}$$

It can also be shown that

$$F = C'R_d \tag{7}$$

Substituting for R_d in eq. (6) yields

$$D_e = D_{e0}C''(1/F) \tag{8}$$

where $C'' = CC'$. Equations (6) and (8) link the rate of composite formation with these monomers to a common characteristic deposition efficiency that is independent of feed composition. Thus R_d appears to be diffusion controlled, at least over much of the preparation range. The magnitude of the constants of eq. (6) (Table III) specify that polymer will deposit only at a high R_d, between 61.6 and 5.5% hr^{-1}; below this rate, where D_e becomes zero, all polymer should form preferentially in the float and on leather surfaces. It may be that a spacial restriction governs the magnitude of both D_e and R_d. In support of this, R_d does correlate fairly well (Fig. 5) with the molar volume of monomer, V_0. It is of special interest that no correlation was found between the solubility of the monomers in water and these parameters. Solubilities at 25°C in water were MMA, 3.0%; BA + MMA, 0.22%; BA, 0.16%. In fact, graft yields and efficiency usually decrease for water soluble monomers, the reverse of the effect found here. With use of the constants of Table III, the limiting molar volume is 238, close to that of *n*-octyl acrylate (209); this monomer was not deposited even in more loosely woven Nigerian sheepskin.[25] However, many more monomers will need to be tested to establish the generality of both D_e and molar volumes as essential parameters.

The limitation of the constant D_e, eq. (4) and Figure 2, is that it expresses only an average value for deposition characteristic of each composite system (see Table I). Thus it is ineffective in monitoring efficiency effects dependent on specific

TABLE III
Constants and Other Quantities in This Work

Equation constants					Density and derived quantities for leathers[a]		
						Average values for leathers	
System	Eq. No.	Slope	Intercept	Symbols	Symbol[b]	Emulsion	Solution
MMA[c]	(4)	0.906	0	D_e	ρ_{a0}	0.5556 ± 0.0273[d]	0.6241 ± 0.0369[d]
BA + MMA[c]	(4)	0.777	0	D_e	V_t	1.799 cm^3	1.602 cm^3
BA[c]	(4)	0.635	0	D_e	V_a	1.103 cm^3	0.9049 cm^3
D_e vs. $1/R_d$	(6)	6.157	1.104	C, D_{e0}	v_{f0}	0.6125	0.5648
MMA	(5)	4.38×10^{-3}	0	F	ρ_r	1.434 g cm^{-3}	1.434 g cm^{-3}
BA + MMA	(5)	2.28×10^{-3}	0	F	A	7.652 cm^b	7.652 cm^b
BA	(5)	1.68×10^{-3}	0	F	h	0.2352 cm	0.2094 cm
F vs. R_d	(7)	1.33×10^{-4}	0	C'	ρ_i	0.6014	
D_e vs. V_0	—	6.59×10^{-3}	1.48	—			
C_p	(27)	1.45			ρ_{a0}/ρ_i	0.9238	

[a] Based on 1 g leather; average values of the apparent densities of approximately 102 samples. Used in computing theoretical curves following eqs. (9)–(27).

[b] The quantities are designated: ρ_{a0}, apparent density; V_t, total volume; V_a, volume of free space; v_{f0}, volume fraction of free space; ρ_r, real density; A, specimen area; h, specimen thickness; ρ_i, average intercept of composite density curve fit, see eq. (19).

[c] Corresponding rate of deposition values R_d obtained from the curve fitted slopes of Figure 3(A), are PMMA, 31.99% hr^{-1}; BA + MMA, 18.17% hr^{-1}; PBA, 13.29% hr^{-1}.

[d] Extreme limiting values were emulsion, 0.5010–0.6150; solution 0.5459–0.6471.

feed composition or time. These are set forth in eq. (2) and are shown graphically in Figures 4(B) and 4(D), as functions of feed, and time, Figure 4(C). All curves are roughly decreasing functions of the variables. The order is MMA > BA + MMA > BA, in harmony with values of D_e (Table III). At very high values of $w_{2\text{feed}}$ ($\geqq 0.5$) efficiencies become very small, especially for batch operations (Table I). Consequently, most of the polymer has formed in the float by the time [Figs. 3(B)–3(D)] 100% conversions are reached. The limits of the bars in the figure indicate much variability in the duplication of individual experiments. This indicates a complex process dependent on variations in the interactions of the leather microstructure, in individual diffusion rates, relative initiator efficiencies, adventitious radical scavenging, and other sources of variability.

Up to this point, the two processes for insertion of polymer into the leather matrix over wide ranges of monomer concentration and time have been scrutinized in considerable detail. However, no information has been made available as to the location of that polymer. The task of locating the polymer in the matrix will be treated in the sections below.

Composite Densities

Consider 1 g (W_1) of leather, free of polymer as shown schematically in Figure 6 (a). From the apparent density (Table III, ρ_{a0}), the total volume V_t is

$$V_t = W_1 w_1 / \rho_{a0} = 1.0/\rho_{a0} \tag{9}$$

The total volume of free space in the leather (i.e., the sum of fine and coarse free space[41]), designated V_a, is given by

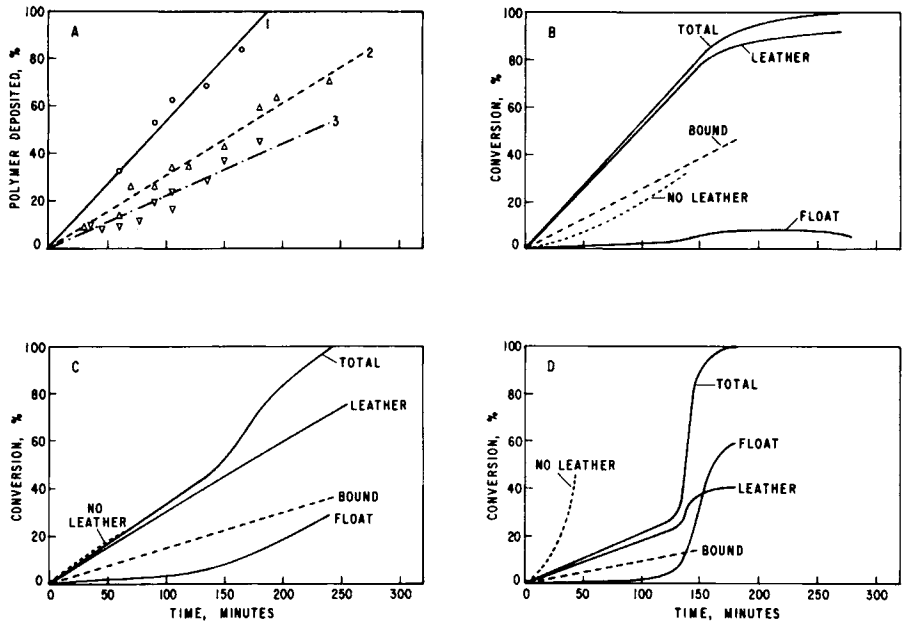

Fig. 3. Rate curves for total polymerization including composite formation using $w_{2\text{feed}} = 0.5$. (A) % polymer deposited in leather vs. time; (1) MMA; (2) BA + MMA; (3) BA. Rate of deposition taken from slopes (Table III). (B, C, D) % conversion–time curves for (B) MMA; (C) BA + MMA; (D) BA. Concentrations were, in ml^{-1}: MMA, $[M]_0 = 1.84$, $[I] = 0.0741$; BA + MMA, $[M]_0 = 1.62$, $[I] = 0.0643$; BA, $[M]_0 = 1.44$, $[I] = 0.0585$, all based on water content.

$$V_a = V_t - V_c \tag{10}$$

where $V_c = 1/\rho_r$ is the volume of collagenous material. The quantity ρ_r is the real density of leather, taken in this work as 1.434 (Table III) as an average of measurements with a helium-air pycnometer on selected controls. This value agrees well with an average value of 1.465[32b] in the literature. Accordingly, the initial volume fraction of free space v_{f0} before any polymer treatment becomes

$$v_{f0} = V_a/V_t = V_a/(V_a + V_c) \tag{11}$$

In composites ($W_1 + W_2$) containing polymer, where the polymer is envisioned to deposit in the fine structure of fibers, as illustrated in Figure 6(b), leather weight fraction w_1 will always be less than unity, and polymer weight fraction w_2 greater than zero. From eqs. (11) and (9), V_a for pure leather will be

$$V_a = V_{a0} = v_{f0}V_{t0} = v_{f0}(W_1w_1/\rho_{a0}) \tag{12}$$

Consequently, apparent densities for all composites containing polymer should follow eq. (13a), or some modification of this equation, as developed in later sections:

$$\rho_a = \frac{W_1 + W_2}{(W_1 + W_2)w_1/\rho_r + (W_1 + W_2)w_2/\rho_p + v_{f0}(W_1 + W_2)w_1/\rho_{a0}} \tag{13a}$$

For composites where $W_1 + W_2 = 1.0$ g, in this and subsequent equations

$$\rho_a = 1/[W_1\rho_r + W_2/\rho_p + v_{f0}(W_1/\rho_{a0})] = v_1\rho_{a0} + v_2\rho_p \tag{13b}$$

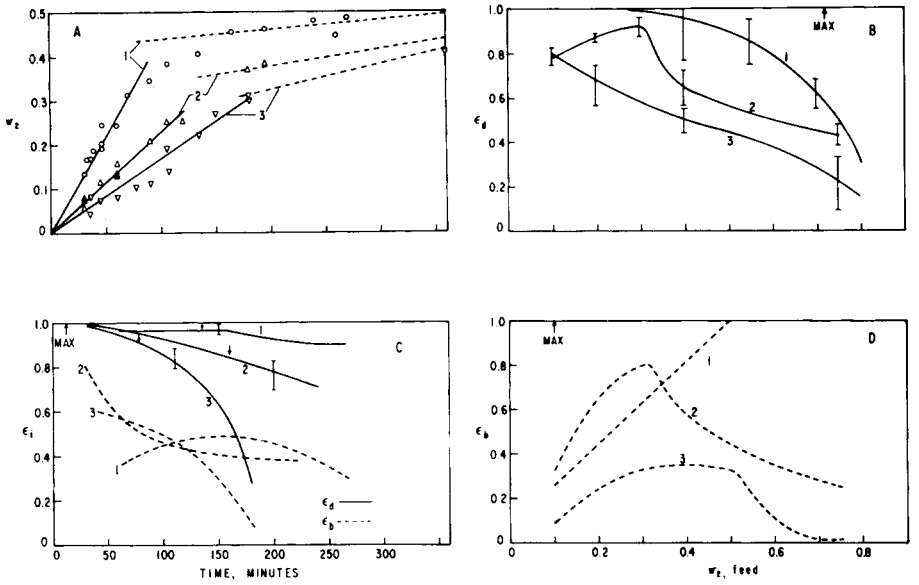

Fig. 4. (A) Rates of formation of w_2 for recipe conditions using $w_{2\text{feed}} = 0.5$. (B) Specific deposition efficiency ϵ_d as a function of $w_{2\text{feed}}$. (D) is the same but using ϵ_b. (C) Comparison of ϵ_d (solid lines) and ϵ_b (dashed lines) as functions of time. Numbers correspond to (1) MMA; (2) BA + MMA; (3) BA. Top of the figure represents the maximum efficiency for (B)–(D). Downward arrows, (C), designate time equivalent to start of steep decent of curves in (B) and (D).

where the subscripts are given in the experimental section. Volume fraction v_i is defined

$$v_2 = \frac{W_2/\rho_p}{W_2/\rho_p + W_1/\rho_a}$$

$$v_1 = 1 - v_2$$

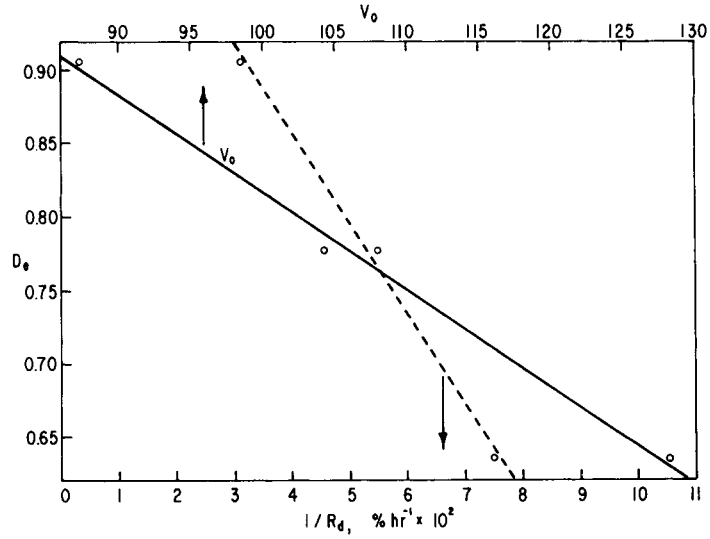

Fig. 5. Relation between the variable feed depositions constant D_e and the reciprocal rate of deposition $1/R_d$, as well as the molar volume of monomers V_0 for the three composite systems.

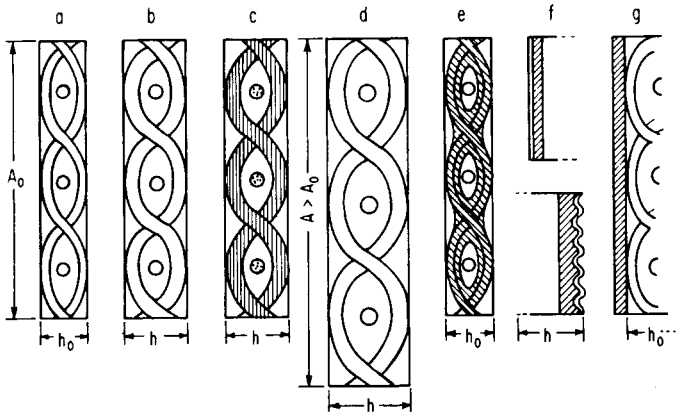

Fig. 6. Idealized models of composites discussed in this work. (a) Base substrate, chrome-tanned 5 oz. cattlehide, acetone dried; (b) polymer deposited from emulsion, eq. (18); (c) same as (b) but after benzene extraction, eq. (17); (d) fibers expanded to preserve initial space, eq. (20); (e) location of bulk or solution polymerized monomers, eq. (21); (f) effect of polymer layer formation in grain (top) and split coriums (bottom) sections, eqs. (22), (23), and (26); (g) surface impregnant, eq. (13).

It immediately follows that specimen volume increases with polymer deposition in accordance with

$$V = \frac{1/W_1}{\rho_a} \tag{14}$$

If only fiber cross sections are expanding [Fig. 6(b)], as most often is found in polymer–fiber composites,[9] then specimen initial length and width will remain constant and specimen thickness becomes

$$h = V/1w = V/A \tag{15}$$

where $1w$ is the initial surface area A_0 cm^2. Finally, from eq. (13a), the volume fraction of free space v_f is obtained as

$$v_f = \frac{V_a}{V_a + V_c + V_p} = \frac{v_{f0}(W_1/\rho_{a0})}{v_{f0}(W_1/\rho_{a0}) + W_1/\rho_r + W_2/\rho_p} \tag{16}$$

Surface impregnants, idealized as model g in Figure 6, should also follow eqs. (13)–(16). Consequently, ρ_a will not distinguish between these types of composites. However because impregnants do enter the leather matrix, presumably into the large pores,[14] density rise for these should be greater than eq. (13a) predicts, as will presently be seen.

Extraction of the composites to remove homopolymer [Fig. 6(c)] will introduce porosity in the fine structure if h and V are unchanged, as was, indeed, observed in this work. Under these conditions, relaxation of the composites cannot have occurred under the influence of solvent and heat. The situation can be described with

$$\rho_a = \{W_1/\rho_r + W_2/\rho_p + [v_{f0}(W_1/\rho_a) + w_h(W_2/\rho_p)]\}^{-1} \tag{17}$$

where w_h is the weight fraction of homopolymer (Table I) removed from the composite, defined $w_h = 1 - (W_b/W_d)$. Thus, eq. (17) accounts for increase in V_a by adding the removed polymer volume to the fractional free space of the density expression, eq. (13b).

When experimental densities (Table I and elsewhere) were inserted on plots of eq. (13b), the data lay just above the theoretical curves. Either the composite shrinks or initially expanded fibers partially fill the free space. By curve fitting the experimental densities for each monomer system with a computer, a small constant correction factor was obtained from the intercept (Table III). The new factor was introduced into eq. (13b) to yield

$$\rho_a = \{W_1/\rho_r + W_2/\rho_p + [v_{f0}(W_1/\rho_{a0})]\rho_{a0}/\rho_i\}^{-1} \tag{18}$$

where ρ_{a0} is the leather density (Table III) and ρ_i the intercept density (Table III) from curve fitting

$$\rho_a = \rho_i + \alpha w_2 + \beta w_2^2 \tag{19}$$

Model d, Figure 6, which can be described by

$$\rho_a = [W_1/\rho_r + W_2/\rho_p + (w_1/V_{a0} + w_2 V_{p0})]^{-1} \tag{20}$$

appears to be highly improbable. Here ρ_a will remain similar to ρ_{a0}. However, it assumes retention of the initial volume fraction of free space by fibrous expansion. Slippage of entangled fibers of cattlehide to allow this appears to be impossible.[14,32b] Moreover, much of the fine pore space in leather[41] is unexpandable. However, some of the experimental composites did show area expansion, in at least partial conformation with the model.

Bulk or solution deposition of polymer into leather (Table II) is described by model e, Figure 6, wherein both fine and coarse pore structure is considered to be incrementally filled with polymer. This can be expressed by

$$\rho_a = \{W_1/\rho_r + W_2/\rho_p + [v_{f0}(W_1/\rho_{a0}) - (W_2/\rho_p)(\rho_r/\rho_p)]\}^{-1} \tag{21}$$

In this expression V_a is incrementally filled with polymer of volume W_2/ρ_p, expanded by the quantity ρ_r/ρ_p. This equation specifies a rapid rise of density with w_2, and, in compliance with the model, that V and h should remain essentially unchanged; that is, $V \approx 1.0$ g/ρ_{a0} and $h \approx h_0$.

An important complication found in this work with densely packed cattlehide used as the substrate but not so readily seen in thinner, looser sheepskin[23–26] is illustrated in Figure 6(f). The deposited polymer is laid down primarily in fibers situated near the outer regions of the matrix, as evidenced by microscope examination of stained sections, producing a sandwich effect of untreated fibers in the center. At small composite loadings ($w_{2\text{feed}} \leqq 0.3$) a clear layer existed at both surfaces (grain and split corium) which could be filled at higher deposition. The combined layers constituted about 25–60% of the specimen cross section. To describe densities having the complication of layering requires a drastic modification of eq. (18). With an assumption of constant layer composition, a general expression for density for layered composites becomes

$$\rho_a = f\left(\frac{1}{W_1/\rho_r} + \frac{W_2}{\rho_p} + \frac{v_{f0}(W_1/\rho_{a0})\rho_{a0}}{\rho_i}\right) + (1 - f)\,\rho_{a0} \tag{22}$$

where f and $1 - f$ are partitioning functions different from the layer fractions. In the polymer composite, layer density ρ_1 can be described by

$$\rho_1 = [W_1'/\rho_r + W_2'/\rho_p + (v_{f0}W_1'/\rho_{a0})(\rho_{a0}/\rho_i)]^{-1} \tag{23}$$

where $w_2 = W_2/(v_2^* + W_2) = (1/W_1 - 1)/[v_2^* + (1/W_1) - 1]$ and $w_1' = 1 - w_2$, with

v_2^* the layer fraction and $W_2 = (1/W_1) - 1 = [(W_1 + W_2)/W_1] - (W_1 + W_2)$ the weight of polymer added to 1 g of leather to make a composite of a designated w_2. Thus, in eq. (23), $W_1' = (W_1 + W_2)w_1'$ and $W_2' = (W_1 + W_2)w_2'$. The coefficients f and $1 - f$ of eq. (22) become

$$f = w_1 = \frac{1}{W_1} - \frac{v_1^*}{1/W_1} = \frac{(W_1 + W_2) - v_1^*}{W_1 + W_2} \tag{24}$$

$$1 - f = w_c = 1 - w_1 \tag{25}$$

so that density is predicted by

$$\rho_a = w_1\rho_1 + w_c\rho_{a0} \tag{26}$$

with the subscript 1 for layer and c for free leather, respectively, and ρ_1 from eq. (23).

The form of eq. (26), in view of eqs. (22) and (23) predicts that the density of layered composites should be indistinguishable from those deposited homogeneously [eq. (18)]. This is analogous to the unchanging density of model g already discussed. Densities of composites estimated by eqs. (18) and (26) were indeed found to be close to curve fitted densities [eq. (19)] for two composite systems (MMA, BA + MMA) for varying w_2 and v_2^* within the experimental range. In the sections below, experimental data are correlated with the above equations; in this way location of the polymer in the matrix can be tentatively established through the extent of statistical adherence of the data to the theoretical models.

Apparent densities as a function of weight fraction of polymer in the composite w_2 are shown for all three composites in Figures 7(A)–7(C). Values for ρ_a calculated from eq. (18) lie close to the curve fitted data [eq. (19)] (dashed line), providing confidence in the validity of eq. (18) as can be seen. The considerable experimental scatter is the result of the variability of densities of the individual leather panels and controls (Table III). This variability is typical of most leathers.[32a] Figure 7(D) compares volumes of MMA composites [eq. (14)] as freshly prepared (curves at top) with those obtained after drying following methanol extractions (dotted line). The fitted curve (dashed line) correlates with a theoretical curve (solid line)

$$V = C_p[(1/W_1)/\rho_a] \tag{27}$$

where $C_p = V_t$ water wet$/V_t'$, where V_t' is $V_t(\rho_{a0}/\rho_i)$, the corrected volume of the initial leather. The wet volume increase by a constant amount ($C_p = 1.451$) over dry volumes indicates that the presence of polymer has little effect in retarding the volume expansion of leather in water. This suggests poor mixing intimacy between polymer and leather phases, thus further denegating a grafting mechanism.

Thickness versus w_2 curves [Figs. 8(A)–8(C)] are described by use of eq. (15) (solid lines) for all three systems and volumes by eq. (14) for MMA composites [Fig. 8(D)]. The experimental points (circles) were obtained by calculation from experimental densities. Measured experimental thickness values (symbol ×) in Figure 8(A) for MMA composites fall close to the values (circles) estimated from density. Similar results were found for the other two systems. This agreement provides evidence that fiber expansion was anisotropic laterally only. Furthermore, since lengthening of fibers and fiber bundles was largely excluded,

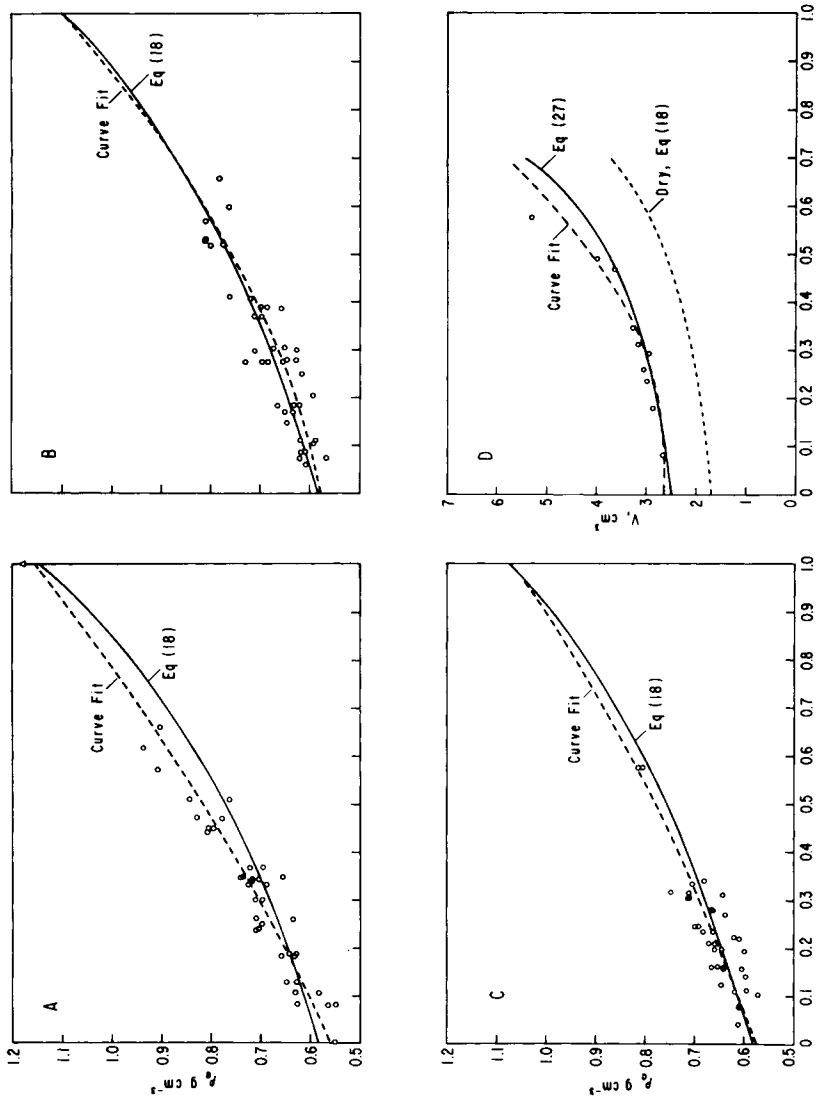

Fig. 7. Apparent density ρ_a vs. w_2 for the polymer deposited composites, prepared by the emulsion technique. (A) MMA; (B) BA + MMA; (C) BA. Comparison, (D), of the volume expansion of as-formed water-wet composites containing MMA and those dried, (A). For all curves, theory, solid line; computer fitted, dashed line, eq. (19).

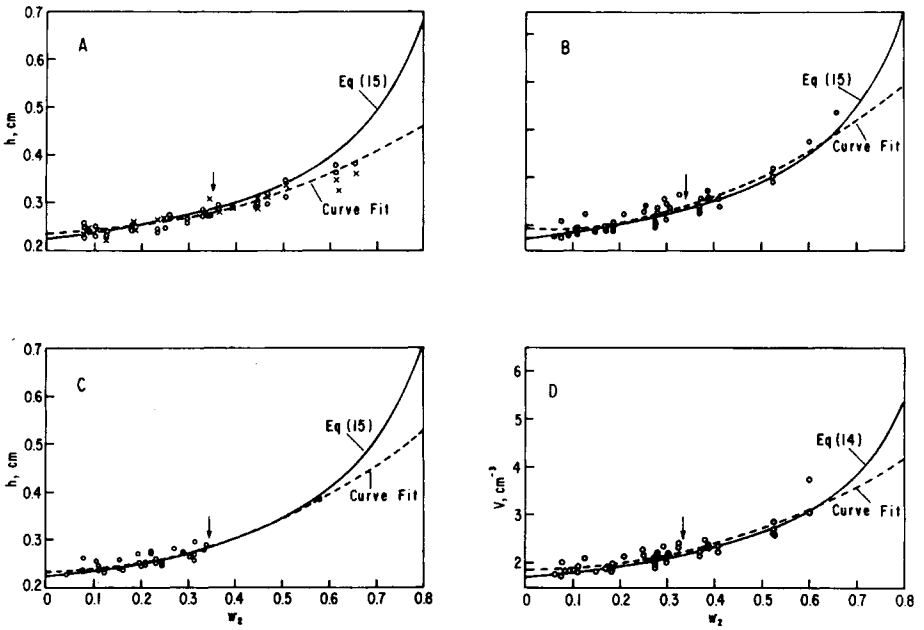

Fig. 8. Thickness h vs. w_2 for the composites prepared by emulsion means. (A) MMA; (B), BA + MMA; (C) BA. Volume V as a function of w_2 for BA + MMA composites (D). Circles computed from experimental densities, symbols marked × are measured thicknesses. Downward arrow marks the equilibrium water plumping equivalent composition. Fitted curves (dashed lines) are of the form of eq. (19).

model d, Figure 6, can be eliminated. Downward arrows mark the composite composition where aqueous plumping equilibria were reached in untreated leathers. Polymer thus adds considerable permanent bulk to the leather, so that natural variability can be effectively obscured,[23–26] but the concentration required is fairly high, $w_2 \approx 0.35$, to even match the plumping produced by pure water in crust cattlehide.[14]

In contrast, the rate of change of density with composition is very much higher for bulk or solution filled systems, as predicted by eq. (21) solid lines and shown in Figures 9(A)–9(C). When the pore space is filled, densities become constant and approach ρ_p for the parent homopolymer. Considerable scatter and a transition region at high ρ_a were found for the experimental points. As predicted, thickness h [eq. (15)] and volume (not shown) remained rather constant, indicating little or no expansion of the fibers, as predicted by eq. (21). The marked differences in the rate of change of free space v_f for emulsion deposited [eq. (16)] and solution polymerized BA + MMA composites is readily seen in Figure 9(D). Since v_f affects comfort in leather by affecting transport of moisture,[32b] the emulsion composites are superior for any predetermined composition [usually $w_2 \approx 0.3$ (refs. 23–26)].

Bound (graft) polymer densities, which should have followed eq. (17) and be sensitive to weight fraction of extractable homopolymer w_h, obviously do not, as can be seen in Figure 10, for three BA + MMA composite systems of varied composition but increasing w_h. Qualitatively, densities fell as predicted but did not fall on the curves. In fact, at high w_h [Fig. 10(C)], densities were lower than predicted and decreased with increase in polymer content. We think that

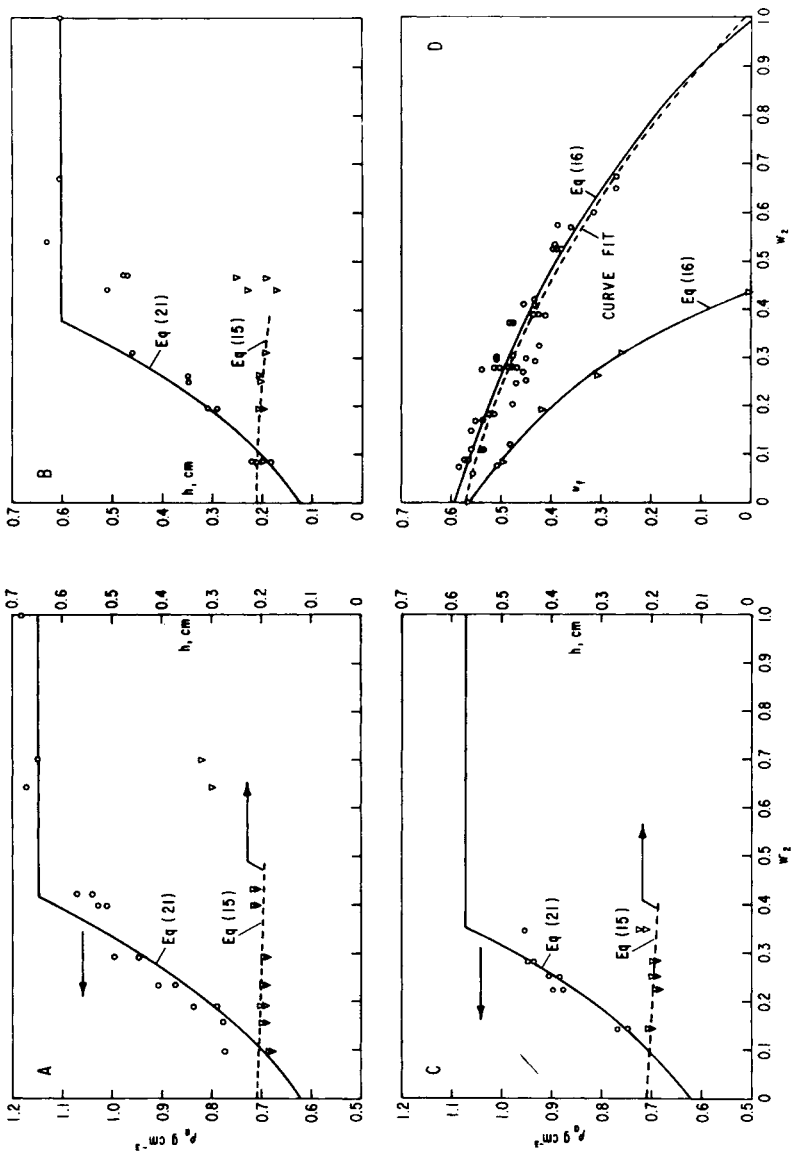

Fig. 9. Apparent density ρ_a and thickness h vs. w_2 for composites prepared by the bulk or benzene solution method. (A) MMA; (B) BA + MMA; (C) BA. Volume fraction of free space v_f vs. w_2 (D) for BA + MMA composites prepared by (a) the emulsion technique and (b) by solution polymerization. Solid lines are theoretical and dashed lines curve fitted [form, eq. (19)].

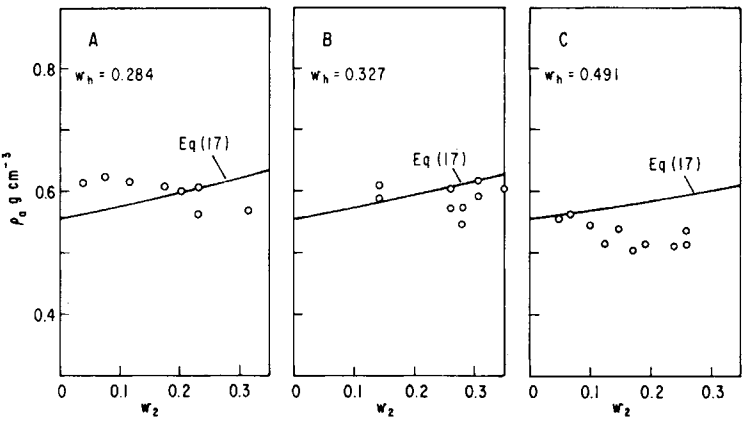

Fig. 10. Apparent density vs. the bound polymer weight fraction w_2 for BA + MMA systems at three average fractional extents of homopolymer removal, expressed as weight fraction homopolymer w_h. Solid line, theoretical curve.

expansion of the polymer domains in the composite with imbibed solvent during benzene extraction produced a destructive and irreversible expansion of the total matrix. Thus, on subsequent drying, densities lower than ρ_{a0} (Table III) could result. This expansion would increase with w_h, as was found in Figure 10. In fact, some highly loaded MMA components became shredded, and thus considerably weakened, after extraction. These observations seem especially important because solvent extraction is the accepted method of isolating grafted polymers in fibers.[7,9,12]

Figure 11 shows the rate of change of the layering fraction v_2^*, with composition [Fig. 11(A)] and time [Fig. 11(B)]. Slash marks denote the composition or time increment when the clear zone became filled; this heralded the onset of gross deposition of polymer in the float [Figs. 3(B)–3(D)]. It appears that polymer initially pervades the leather through a fixed volume fraction of fibers, leaving a clear zone at the surfaces, and builds in both directions, resulting, just before transfer of polymerization activity to the float, in an expanded final layer v_2^*.

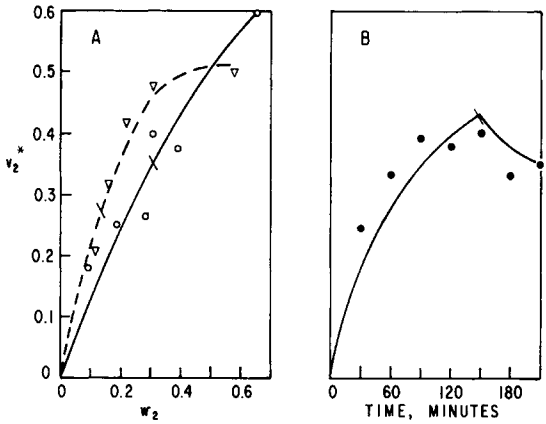

Fig. 11. Variation of apparent layering fraction v_2^* with polymer deposition weight fraction w_2 (A), and time (B) for composites of BA + MMA, solid lines and BA, dashed line. Slash marks denote the region of disappearance of the clear zone and the beginning of an embedded appearance.

Molecular Weight Data

Table IV lists number-average molecular weights for selected emulsion prepared bound, deposited, and float polymers collected in this work; bound polymer frequencies, eq. (3); and the number of amino acids per branch chain length $P/\overline{DP}_n$. Molecular weights were usually higher for polymers either bound or deposited in the leather than for polymers forming in the float. Thus, the usual behavior indicating a reduction of the chain termination constant k_t as the result of gel effect that was observed by most other authors[7,9,36–38,42,43] appears to be present here. The relatively small values of $\overline{M}_n$ for the deposited and bound polymers isolated from the BA composites apparently reflect a long low-molecular-weight tail in their molecular weight distributions. Viscosity-average molecular weights, which favor the largest species present, were 816,000 and 793,000 for experiments 17 and 18, respectively. This implies high values of $\overline{M}_n$ for the others in the monomer group. A specific pattern for $\overline{M}_n$ as a function of composition in each group is noticeably absent. Of course, trends may be obscured by variable molecular weight distributions. However, bound polymer frequencies F_b increase incrementally with feed composition in each monomer group. However, values of F_b are always appreciably less than maximum values $F_{b\max}$, the latter being computed on the basis of complete initial feed conversion to bound polymer of the experimental molecular weights. This may be seen more clearly (Fig. 12) when their ratios $F_b/F_{b\max}$, taken as indices of bound polymer efficiency, are compared with accurate values of efficiency $w_b/w_{2\text{feed}}$, where w_b is the bound polymer weight fraction. Although data for all three composite systems fell on the same curve, the coefficient 1.108 is greater than unity and the intercept (−0.1542) is not the origin. Increasing bound polymer inefficiency (right to left and top to bottom in Fig. 12) occurs as feed composition is increased for both parameters but is more severe for the frequency data. According to eq. (3), grafting frequency should increase exponentially with increasing feed composition, at fixed graft polymer molecular weight, thus requiring ever increasing graft branches to maintain $F_b/F_{b\max}$ at unity. Far from $F_b/F_{b\max}$ maintaining unity with increasing monomer concentration, the index values are even depressed relative to $w_b/w_{2\text{feed}}$, indicating extremely rapid depletion of assumed grafting sites. Similar trends have been found by other workers.[7,9,36–38,42,43] This is difficult to reconcile with the premise of a controlling grafting mechanism for polymer deposition, regardless of method.[7,9,12] In the absence of predominant grafting, the observed trends in bound polymer frequencies could simply reflect a mechanism requiring reduced polymer deposition in individual fibers that is relatively insensitive to feed composition. A precipitation mechanism involving transport of monomer to occluded radicals is compatible with this concept.

Such a mechanism may be qualitatively envisioned as pictured schematically in Figure 13. Each insert represents an assembly of fibers positioned at various depths in the layered regions (defined by braces) of polymer deposition. Insert 1 shows radicals (dots) being generated at the commencement of polymerization from the redox couples preferentially adsorbed on and near fibrils. Preferential adsorption has been observed for initiators on cotton,[44,45] wool,[9] and collagen.[26] The initial deposition region in the leather panels should be determined by the sorbed persulfate concentration gradient, which fixes the layer by polymerizing the initially available monomer. This layer will increase in leathers having de-

TABLE IV
Molecular Weights and Bound Polymer Frequencies for the Emulsion-Prepared Composites

Experiment No.[a]	System	Molecular weights $\overline{M}_n$ bound	$\overline{M}_n$ deposited	$\overline{M}_n$ float	F_b	$F_{b\max}$	$F_b/F_{b\max}$	$w_b/w_{2\text{feed}}$	$P/\overline{DP}_n$[b] bound	$w_{2\text{feed}}$
1	MMA			195,050[c]						
2	MMA	348,300	360,700		0.084	0.215	0.393	0.447	25.1	0.200
6	MMA	195,500			0.294	3.07	0.096	0.241		0.667
3	MMA	309,200	531,600		0.247	0.418	0.591	0.674	9.27	0.301
7	MMA	191,800			0.421	4.69	0.090	0.283		0.750
4	MMA	522,400	541,100		0.289	0.384	0.751	0.834	15.7	0.401
5	MMA	541,100	1,045,000		0.448	0.554	0.808	0.894	16.2	0.500
8′				168,350[c]						
9	BA + MMA	492,400		312,400[d]	0.0993	0.152	0.652	0.701	5.24[g]	0.200
10	BA + MMA	605,300		606,000[d]	0.174	0.212	0.818	0.865	14.5[g]	0.300
11	BA + MMA	592,900	891,200	242,400	0.195	0.339	0.577	0.697	3.49[g]	0.401
12	BA + MMA	1,263,200	918,200	505,000	0.105	0.238	0.441	0.612	4.84[g]	0.500
13	BA + MMA	1,162,100	365,100	140,950	0.141	0.775	0.182	0.471	1.27[g]	0.750
15′	BA			199,200[c]						
15	BA	484,200		294,600[e]	0.0416	0.155	0.269	0.315	36.9[g]	6.200
16	BA	181,600		239,700[e]	0.154	0.708	0.218	0.284	45.6[g]	0.300

17	BA	299,500		257,100[e]	0.210	0.668	0.315	0.433	9.25[g]	0.400
18	BA	264,200		404,000[e]	0.398	1.14	0.350	0.519	11.6[g]	0.500
19	BA		229,900	157,100[e]					4.00[h]	
20	BA		277,300						3.66[h]	0.750
21′	BA + MMA rate	744,300		189,400[f]	0.0339	0.0469	0.723	0.742	0.104[e]	
22′	BA + MMA rate	883,800			0.0445	0.0595	0.748	0.776		0.149[e]
23′	BA + MMA rate	565,600	522,400		0.134	0.157	0.855	0.884	36.6[h]	0.228[e]
24′	BA + MMA rate	471,400	606,000		0.136	0.180	0.757	0.799		0.221[e]
25′	BA + MMA rate	883,800	739,000		0.106	0.145	0.729	0.794	74.0[h]	0.299[e]
26′	BA + MMA rate	642,800	522,400	300,000	0.141	0.219	0.643	0.726	26.6[h]	0.320[e]
27′	BA + MMA rate	479,300	473,400	303,000	0.290	0.431	0.673	0.776	32.9[h]	0.408[e]

[a] Numbers correspond to those in Table I; primed numbers are new experiments.

[b] $P \approx \{[5.62(\%\ N/100)]/93.75\}(1/\overline{M}_n)$, where 93.73 is taken as the average molecular weight of the amino acid groups present. 5.62 is the conversion factor for N to hide substance.

[c] Control, no leather, same $[I] = 0.04$ mole fraction monomer.

[d] Air dried.

[e] Emulsion, MeOH extracted, experiments 18–22, Table I.

[f] w_2 deposited polymer, 0.0612.

[g] Float polymer only.

[h] Deposited polymer only.

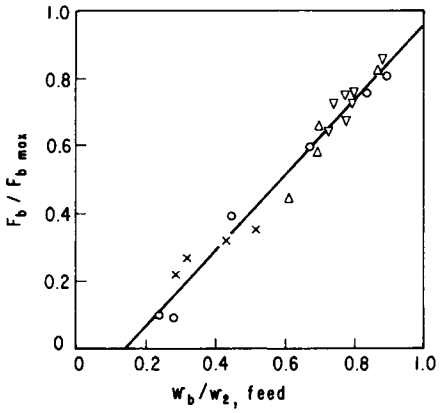

Fig. 12. Quantity F_b/F_{bmax} vs. w_b/w_{2feed} for all three composite systems. Circles, MMA; triangles, BA + MMA; ▽, BA + MMA rate; ×, BA.

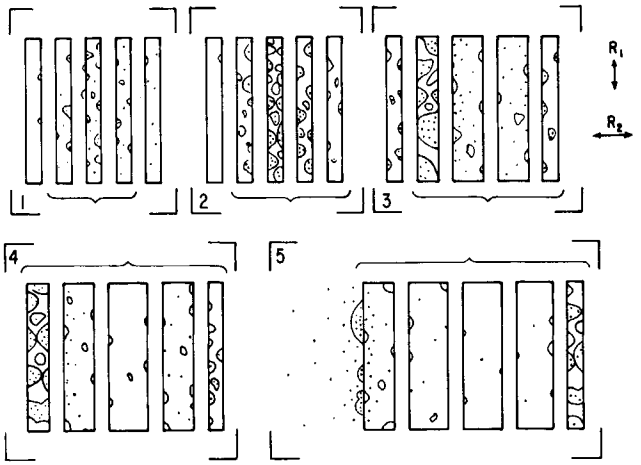

Fig. 13. Schematic diagrams representing the deposition of polymer in leather as a function of time [time increasing, (1)–(5)]. Diagram represents individual fibers selected at different positions in the layered region v_2^* (the region in braces). The extreme left fiber in (1)–(3) is the clear zone at the surfaces. Dots represent active centers. R_1 is the rate of fiber filling; R_2 is the rate of layer expansion. R_1 exceeds R_2 in (1)–(3) but is exceeded by R_2 in (4) and (5).

creased fiber density. Thus less tightly packed sheepskin[23–26] and collagen powder[19–22] received more polymer, and the intact leathers were filled more homogeneously.

Following initiation, nucleation of polymer aggregates commences. These grow (Fig. 13, inserts 2 and 3), with eventual fusion of aggregate and expansion of fibers. Occluded active centers add increasingly to those being generated in the aqueous phase as polymer precipitates; propagating macroradicals are fed by monomer diffusing through the polymer phase and depositing on the surfaces of aggregates. Thus, diffusion appears to control the rate of deposition. The role of surfactant will be treated in the next paper.[1a] As the surface to volume ratio of the expanding fibers decrease, the center of polymerization changes (Fig. 13, inserts 3 and 4); fibers more distant from the initial layer commence filling, thus expanding the layers. However, fibers located in the clear zones should

be filled at rates faster than those inside because the time for monomer diffusion is shorter. Finally, electrolyte and active center populations will be largely transferred to the external float, where polymerization will continue at a very rapid rate, induced by the net increase in active centers, to complete the conversion of monomer (Fig. 3). Bound polymer in this scheme should result mostly from termination of branched macroradicals and from severe restrictive entanglements in the tightly packed fibrillar matrix, causing extremely slow rates of solvent removal.[12] We observed that the effect of successive extraction of the composites by a large excess of hot benzene for long times was a very slow approach to an asymptotic limit of polymer removed. In addition, many of the extracted polymers (labeled deposited) in Table IV had considerable (20–50%) microgel, which was removed by filtration.

In the above qualitative outline, no explanation is presently available for the initial creation of a clear zone (Fig. 6). Also unknown is an explanation for the large differences in rates of deposition (Fig. 3) for the three monomers. However, work to be presented in the next manuscript attempts to provide some of these answers.[1a]

In principle, analysis by end group, together with molecular weights of grafted branches isolated by dilute hydrochloric acid digestion, should provide both proof of grafting[9,19,28] and information regarding the mechanism of termination.[9] However, data in column 10 of Table IV show such a plurality of amino acids for each polymer chain and so many variable results for each $\overline{DP}_n$ unit of the bound polymer that no conclusion can be reached on either point. More significantly, extractable and even float polymer showed similar results. The low sensitivity of the nitrogen analysis in counting small numbers of amino acids, in combination with contamination with residual nitrogenous material, may have produced the observed results. However, even when greater care was taken in the isolation and identification, integer values greater than 2 (ref. 9) were sometimes[28] but not always[19] found.

SUMMARY AND CONCLUSIONS

Three different monomer systems over wide ranges in composition were polymerized into the fibrous matrix of cattlehide by a standard persulfate-bisulfite emulsion type process developed at this laboratory. The monomers were methyl methacrylate, a mixture of *n*-butyl acrylate and methyl methacrylate (containing 0.53 mole fraction of *n*-butyl acrylate), and *n*-butyl acrylate. These were selected to provide the widest range of variation of T_g to the composites. The same monomers were also introduced into the pores of leather by a bulk or solution polymerization with AIBN employed as the initiator. Polymer deposition by the aqueous emulsion method was analyzed as a function of both feed composition at 100% conversion and time at fixed high feed concentration. Overall deposition was proportional to a characteristic deposition rate; below a critical rate of about 6% hr^{-1} no deposition of acrylates was predicted to occur. Deposition order was methyl methacrylate > comonomer > *n*-butyl acrylate. However, individual deposition efficiencies for composition and time variables decreased roughly monotonically. Information on polymer location by both methods of polymer deposition came from successful correlation of experimental densities with theoretical models. A qualitative picture for the aqueous process

finally emerged that considered low grafting frequency values obtained. Polymer deposition appears to be nucleated by adsorbed persulfate bisulfite redox initiator but grows in external layers largely by an occluded radical precipitation mechanism to saturate and expand the microfine porous fibrillar region of the leather. Polymerization activity is then largely transferred to the external aqueous region. Graft polymerization, therefore, does not seem to be the dominant mechanism in these systems.

The authors express their special thanks to Mrs. Sandra P. Graham, Northeastern Region, Agricultural Research, Science and Education Administration, USDA, for the operation of the computer, and thank Joseph W. Cheskiewicz, Hides and Leather Laboratory, ERRC, for some of the nitrogen determinations.

References

1. (a) E. F. Jordan, Jr., B. Artymyshyn, A. L. Everett, M. V. Hannigan, and S. H. Feairheller, *J. Appl. Polym. Sci.*, (Part II) to appear; (b) *J. Appl. Polym. Sci.*, (Part III) to appear; (c) *J. Appl. Polym. Sci.*, (Part IV) to appear.

2. K. Panduranga Rao, K. Thomas Joseph, and Y. Nayudamma, *J. Sci. Ind. Res.*, **29**(12), 559 (1970).

3. K. Panduranga Rao, K. Thomas Joseph, Y. Nayudamma, and M. Santappa, *J. Sci. Ind. Res.*, **33**(5), 243 (1974).

4. G. M. Brauer and D. J. Termini, *Adv. Chem. Ser.*, **145**, 175 (1975).

5. S. M. Atlas and H. Mark, *Cellul. Chem. Technol.*, **3**, 325 (1969).

6. J. C. Arthur, *J. Macromol. Sci. Chem.*, **5**, 1057 (1970).

7. J. C. Arthur, *Adv. Macromol. Chem.* **2**, 1 (1970).

8. M. S. Bains, *J. Polym. Sci., Part C*, **37**, 125 (1972).

9. K. Arai, *Block and Graft Copolymerization*, R. J. Ceresa, Ed., Wiley, New York, 1973, pp. 193–310.

10. W. J. Wasley, in ref. 9, pp. 311–333.

11. P. J. Nayak, *J. Macromol. Sci. Rev. Macromol. Chem.*, **14**(2), 193 (1976).

12. I. C. Watt, *J. Macromol. Sci. Rev. Macromol. Chem.*, **5**(1), 175 (1970).

13. (a) G. N. Ramachondran, Ed., *Treatise on Collagen*, Academic, New York, 1967, pp. 103–183; (b) A. J. Hodge, ibid., pp. 185–205.

14. T. Thorstensen, *Practical Leather Technology*, Krieger, Huntington, NY, 1976.

15. I. V. Yannas, *J. Macromol. Sci. Rev. Macromol Chem.*, **7**(1), 49 (1972).

16. J. C. W. Chien, *J. Macromol. Sci. Rev. Macromol Chem.*, **12**(1), 1 (1975).

17. K. Panduranga Rao, K. Thomas Joseph, and Y. Nayudamma, *Leather Sci. (Madras)*, **14**, 73 (1967).

18. K. Panduranga Rao, K. Thomas Joseph, and Y. Nayudamma, *Leather Sci. (Madras)*, **16**, 401 (1969).

19. K. Panduranga Rao, K. Thomas Joseph, and Y. Nayudamma, *J. Polym. Sci. Part A-1*, **9**, 3199 (1971).

20. K. Panduranga Rao, K. Thomas Joseph, and Y. Nayudamma, *J. Appl. Polym. Sci.*, **16**, 975 (1972).

21. K. Panduranga Rao, K. Thomas Joseph, and Y. Nayudamma, *Leather Sci. (Madras)*, **19**, 27 (1972).

22. K. Panduranga Rao, D. H. Kamat, K. Thomas Joseph, M. Santappa, and Y. Nayudamma, *Leather Sci. (Madras)*, **21**, 111 (1974).

23. A. H. Korn, S. H. Feairheller, and E. M. Filachione, *J. Am. Leather Chem. Assoc.*, **67**, 111 (1972).

24. A. H. Korn, M. M. Taylor, and S. H. Feairheller, *J. Am. Leather Chem. Assoc.*, **68**, 224 (1973).

25. E. H. Harris, M. M. Taylor, and S. H. Feairheller, *J. Am. Leather Chem. Assoc.*, **69**, 182 (1974).

26. M. M. Taylor, E. H. Harris, and S. H. Feairheller, *J. Am. Leather Chem. Assoc.*, **72**, 294, (1977).

27. K. Satish Babu, K. Panduranga Rao, K. Thomas Joseph, M. Santappa, and Y. Nayudamma, *Leather Sci. (Madras)*, **21**, 353 (1974).

28. H. A. Gruber, E. H. Harris, and S. H. Feairheller, *J. Appl. Polym. Sci.*, **21**, 3465 (1977).

29. E. H. Harris and S. H. Feairheller, *Polym. Eng. Sci.*, **17**, 287 (1977).

30. M. M. Taylor, E. H. Harris, and S. H. Feairheller, *Polym. Prepr. Am. Chem. Soc. Div. Polym. Chem.*, **19**(1), 618 (1978).

31. C. M. Brauer and D. J. Termini, *J. Biomed. Mater. Res.*, **8**, 451 (1974).

32. (a) J. Mandel and J. R. Kanagy, *Chemistry and Technology of Leathers*, Vol. 4, F. O. Flaherty, W. T. Roddy, and R. M. Lollar, Eds., Reinhold, New York, 1965, pp. 223–242; (b) J. Kanagy, ibid., pp. 369–416.

33. (a) J. Brandrup and E. H. Immergut, Eds., *Polymer Handbook*, Interscience, New York, 1966, pp. III–66–III–69; (b) ibid., pp. II–353–II–358.

34. E. F. Jordan, Jr., G. R. Riser, C. Salber, and A. N. Wrigley, *J. Appl. Polym. Sci.*, **16**, 3017 (1972).

35. D. W. Van Krevelin and P. J. Hoftyzer, *J. Appl. Polym. Sci.*, **13**, 871 (1969).

36. R. Y. M. Huang and P. Chandramouli, *J. Appl. Polym. Sci.*, **12**, 2549 (1968).

37. R. Y. M. Huang and W. H. Rapson, *J. Polym. Sci. Part C*, **2**, 169 (1963).

38. R. Y. M. Huang, *J. Appl. Polym. Sci.*, **10**, 325 (1966).

39. H. A. J. Battaerd and G. W. Tregear, *Graft Copolymers*, Interscience, New York, 1967, pp. 18, 19.

40. Z. Reyes, C. E. Rist, and E. R. Russel, *J. Polym. Sci. Part A-1*, **4**, 1031 (1966).

41. R. R. Stromberg and M. Swedlow, *J. Am. Leather Chem. Assoc.*, **50**, 336 (1955).

42. R. Y. M. Huang and P. Chandranouli, *J. Polym. Sci. Part A-1*, **7**, 1393 (1969).

43. R. Y. M. Huang, B. Immergut, E. H. Immergut, and W. H. Rapson, *J. Polym. Sci. Part A, 1*, 1257 (1963).

44. Y. Ogiwara, Y. Ogiwara, and H. Kubota, *J. Polym. Sci. Part A-1*, **6**, 1489 (1968).

45. Y. Ogiwara, H. Kubota, and Y. Ogiwara, *J. Polym. Sci. Part A-1*, **6**, 3119 (1968).

Received October 18, 1979
Accepted February 29, 1980